An equilibrium for frustrated quantum spin systems in the stochastic state selection method

An equilibrium for frustrated quantum spin systems in the stochastic state selection method

Tomo Munehisa and Yasuko Munehisa

Faculty of Engineering, University of Yamanashi, Kofu 400-8511, Japan

E-mail: munehisa@yamanashi.ac.jp

Abstract
We develop a new method to calculate eigenvalues in frustrated quantum spin
models. It is based on the stochastic state selection (SSS) method, which is
an unconventional Monte Carlo technique that we have investigated in recent
years. We observe that a kind of equilibrium is realized under some conditions
when we repeatedly operate a Hamiltonian and a random choice operator, which
is defined by stochastic variables in the SSS method, to a trial state. In this
equilibrium, which we call the SSS equilibrium, we can evaluate the lowest
eigenvalue of the Hamiltonian using the statistical average of the normalization
factor of the generated state.

The SSS equilibrium itself has already been observed in unfrustrated
models. Our study in this paper shows that we can also see the equilibrium in
frustrated models, with some restriction on values of a parameter introduced in
the SSS method. As a concrete example, we employ the spin-1/2 frustrated J_1–
J_2 Heisenberg model on the square lattice. We present numerical results on the
20-, 32-, and 36-site systems, which demonstrate that statistical averages of the
normalization factors reproduce the known exact eigenvalue to good precision.
Finally, we apply the method to the 40-site system. Then we obtain the value of
the lowest energy eigenvalue with an error of less than 0.2%.

1. Introduction

The quantum Monte Carlo method is well established in the numerical study of quantum
spin systems. This method has given us fruitful results for understanding the properties
of unfrustrated systems, especially of the spin-1/2 quantum Heisenberg anti-ferromagnet on
bipartite lattices [1]. But, due to the so-called sign problem, the method is not useful for studies
of frustrated systems. In contrast to this, the exact diagonalization is applicable even when
systems are frustrated. Using this method, however, one can only deal with systems on small-
sized lattices. In order to overcome this difficulty, lots of active studies for numerical methods
have been made using the Monte Carlo approach. Among them, the renormalization group

method [2] and the reconfiguration method combined with the fixed-node method [3] are quite noticeable. Also, the extension of the density matrix renormalization group method [4] is worth noting.

Recently we have developed a new Monte Carlo method for evaluating the energy eigenvalues of quantum spin systems [5–9]. We call it the *stochastic state selection* (SSS) method[1]. This method provides an essential improvement on early attempts to truncate the Hilbert space by omitting small values of coefficients [10]. *Not* being based on importance samplings, the method enables us to select a relatively small number of states from a vast full vector space. This selection is simple and is mathematically justified, so one can calculate correct values of inner products through statistical averaging processes. In order to realize this selection, we employ an operator which we call the *random choice operator*. This operator is represented by a diagonal matrix whose elements are stochastic variables with unit averages.

It is possible to combine the SSS method with various techniques for numerical studies. For instance, several applications with the power method are in [6, 7]. By repeating alternate operations of the random choice operator and the Hamiltonian to a trial state, we demonstrated numerically that we can obtain expectation values for powers of the Hamiltonian even when limited computer memory resources are available. We have also combined the SSS method with the Lanczos method in order to obtain the lowest energy eigenvalue of the spin-$1/2$ quantum Heisenberg anti-ferromagnet on the triangular lattice up to 48 sites [9]. It should be noted that these applications of the SSS method are simple from mathematical points of view, because the statistical averaging process for random variables is clear.

In this paper we discuss another application of the SSS method that is essentially different from the applications stated above. Here we consider a number of intermediate states which are successively generated by the random choice operator and an operator related to the Hamiltonian, and measure their normalization factors. Generally, the standard deviation of the inner product between the initial trial state and the Lth generated state increases as L grows. In some conditions, however, the deviation does not increase but becomes constant when L goes beyond some value. We call this phenomenon an *equilibrium*, because in this situation statistical averages of the inner product do not depend on L after suitable normalizations. This type of equilibrium is quite interesting since, from values of the normalization factor, one can obtain the lowest energy eigenvalue precisely and simply. We first observed such phenomena in our study of the J_1–J_2 Heisenberg model with unfrustrated[2] couplings [8].

In this paper we study the equilibrium in the frustrated case. From qualitative discussions we show that the equilibrium for frustrated systems exists in some parameter region. A concrete example for numerical examinations is the spin-$1/2$ J_1–J_2 Heisenberg model on the square lattice with couplings $J_1 = 1$ and $J_2 = 0.5$, the model which is one of the most popular frustrated models with ample numerical results [11–15]. Studying this model up to 40 sites, we find that our results give tangible evidence for the equilibrium.

This paper is organized as follows. The next two sections are devoted to definitions and qualitative discussions. In section 2, after brief descriptions of the SSS method, a definition of the SSS equilibrium is given. Here we also explain why the equilibrium enables us to calculate the lowest energy eigenvalue. Section 3 summarizes discussions on where the equilibrium takes place. We briefly repeat our previous argument [8] with which we concluded that the equilibrium should appear in any unfrustrated system. Then we argue that, for frustrated systems, the equilibrium also exists in some parameter region. In section 4 we present

---

[1] The original SSS method used in [5, 6] is now replaced by the recursive SSS (RSSS) method which has been proposed in [7]. Therefore we refer to the recursive SSS method as the SSS method in this paper.
[2] In a previous paper [8] we state that the model is non-frustrated when $J_2/J_1 = 0$. In this paper we call both the $J_2/J_1 < 0$ and the $J_2/J_1 = 0$ cases unfrustrated.

numerical results on the frustrated J_1–J_2 Heisenberg model. We first direct our attention to the model on a 20-site lattice. On this small lattice it is easy to obtain the exact ground state by the diagonalization method. Consequently, we can directly measure overlaps between the exact ground state and the states generated through stochastic state selections. Note that, as is discussed in section 2, those overlaps are most effective to prove the existence of the SSS equilibrium. In the 20-site case it is also possible to make detailed observations on several quantities introduced in section 3. In section 4.1 we will show that assumptions that we employ in section 3 are mostly reasonable for the model and that the eigenvalue that we obtain through normalization factors is in good agreement with the exact ground-state energy. We also examine how many basis states are needed in our method to calculate the eigenvalue with enough precision. Section 4.2 presents our results for the 32- and 36-site systems. For these sizes we construct bases taking some symmetries into account. Without knowing the exact ground state, we use not overlaps but normalization factors to observe the SSS equilibrium in these systems. Our results indicate that the eigenvalues that we calculate in the equilibrium nicely reproduce the exact ground-state energies reported in [11]. In section 4.3 we present results for the 40-site system. The final section is devoted to a summary and discussion.

2. Stochastic state selection equilibrium

First we briefly review the SSS method [7]. Consider a system whose Hamiltonian is $\hat{H}$ and suppose that its full vector space is given by a basis $\{|i\rangle\}$ ($i = 1, \ldots, N_V$). Here N_V denotes the size of the full vector space. We denote the lowest energy eigenvalue of $\hat{H}$ by E and its eigenstate by $|\psi_E\rangle$. For convenience, a new notation $\hat{Q}$ is used hereafter,

$$\hat{Q} \equiv l\hat{I} - \hat{H}, \tag{1}$$

with the identity operator $\hat{I}$ and a positive number l. Since the present method is based on the power method, the value of l should be chosen to ensure that $Q \equiv l - E(>0)$ is the largest among absolute values of eigenvalues for $\hat{Q}$.

Let us employ a normalized trial state $|\psi^{(0)}\rangle \equiv \sum_i |i\rangle c_i^{(0)}$, $\langle\psi^{(0)}|\psi^{(0)}\rangle = 1$. We introduce random choice operators

$$\hat{M}_{\{\eta^{(m)}\}} = \sum_{i=1}^{N_V} |i\rangle \eta_i^{(m)} \langle i| \qquad (m = 1, 2, \ldots), \tag{2}$$

in order to calculate

$$\hat{Q}\hat{M}_{\{\eta^{(L)}\}} \hat{Q}\hat{M}_{\{\eta^{(L-1)}\}} \cdots \hat{Q}\hat{M}_{\{\eta^{(1)}\}} |\psi^{(0)}\rangle \tag{3}$$

instead of $\hat{Q}^L|\psi^{(0)}\rangle$, the state which would become close to $(l - E)^L|\psi_E\rangle$ for large values of L. The random variable $\eta_i^{(m)}$ in (2) is generated following the *on–off probability function* $P_i^{(m)}(\eta)$. Using a positive parameter ϵ and the coefficient $c_i^{(m-1)}$ in the normalized intermediate state $|\psi^{(m-1)}\rangle \equiv \sum |i\rangle c_i^{(m-1)}$, which is proportional to $\hat{Q}\hat{M}_{\{\eta^{(m-1)}\}} \cdots \hat{Q}\hat{M}_{\{\eta^{(1)}\}} |\psi^{(0)}\rangle$, we define

$$P_i^{(m)}(\eta) \equiv \frac{1}{a_i^{(m)}} \delta(\eta - a_i^{(m)}) + \left(1 - \frac{1}{a_i^{(m)}}\right)\delta(\eta), \qquad \frac{1}{a_i^{(m)}} \equiv \min\left(1, \frac{|c_i^{(m-1)}|}{\epsilon}\right). \tag{4}$$

Then, starting from a given $|\psi^{(0)}\rangle$, we sequentially calculate

$$|\psi^{(m)}\rangle \equiv \hat{Q}\hat{M}_{\{\eta^{(m)}\}} |\psi^{(m-1)}\rangle / C^{(m)} \tag{5}$$

for $m = 1, 2, 3, \ldots$, where $C^{(m)}$ (>0) is the normalization factor determined by

$$[C^{(m)}]^2 = \langle\psi^{(m-1)}| \hat{M}_{\{\eta^{(m)}\}} \hat{Q}^2 \hat{M}_{\{\eta^{(m)}\}} |\psi^{(m-1)}\rangle. \tag{6}$$

We also define a *random state* $|\chi^{(m)}\rangle g^{(m)}$ with the normalization condition $\langle\chi^{(m)}|\chi^{(m)}\rangle = 1$ by

$$|\chi^{(m)}\rangle g^{(m)} \equiv \hat{M}_{\{\eta^{(m+1)}\}}|\psi^{(m)}\rangle - |\psi^{(m)}\rangle = \sum_i |i\rangle c_i^{(m)}(\eta_i^{(m+1)} - 1). \tag{7}$$

It should be kept in mind that, for any state $|\Phi\rangle \equiv \sum |i\rangle b_i$ with b_i s irrelevant to $\{\eta_i^{(m+1)}\}$, the statistical average of the inner product between $|\Phi\rangle$ and this random state is zero,

$$\langle\!\langle\langle\Phi \mid \chi^{(m)}\rangle g^{(m)}\rangle\!\rangle = 0, \tag{8}$$

because

$$\langle\!\langle\eta_i^{(m+1)}\rangle\!\rangle \equiv \int_0^\infty \eta_i^{(m+1)} P_i^{(m+1)}(\eta_i^{(m+1)}) \, \mathrm{d}\eta_i^{(m+1)} = 1, \tag{9}$$

from (4).[3] Also remember that

$$\langle\!\langle[g^{(m)}]^2\rangle\!\rangle = \left\langle\!\left\langle\sum_i [c_i^{(m)}]^2(\eta_i^{(m+1)} - 1)^2\right\rangle\!\right\rangle = \sum_{0<|c_i^{(m)}|<\epsilon} [c_i^{(m)}]^2\left(\frac{\epsilon}{|c_i^{(m)}|} - 1\right)$$

$$= \epsilon \sum_{|c_i^{(m)}|<\epsilon} |c_i^{(m)}| - \sum_{|c_i^{(m)}|<\epsilon} [c_i^{(m)}]^2, \tag{10}$$

where we use (9) and

$$\langle\!\langle[\eta_i^{(m+1)}]^2\rangle\!\rangle \equiv \int_0^\infty [\eta_i^{(m+1)}]^2 P_i^{(m+1)}(\eta_i^{(m+1)}) \, \mathrm{d}\eta_i^{(m+1)} = a_i^{(m+1)}. \tag{11}$$

Now we define the SSS equilibrium.[4] We divide the intermediate state $|\psi^{(m)}\rangle$ into a part which is proportional to $|\psi_E\rangle$ and the rest,

$$|\psi^{(m)}\rangle = |\psi_E\rangle w^{(m)} + |\zeta^{(m)}\rangle s^{(m)}. \tag{12}$$

Here

$$w^{(m)} \equiv \langle\psi_E|\psi^{(m)}\rangle \tag{13}$$

and

$$|\zeta^{(m)}\rangle s^{(m)} \equiv |\psi^{(m)}\rangle - |\psi_E\rangle w^{(m)} \tag{14}$$

with the normalization condition $\langle\zeta^{(m)}|\zeta^{(m)}\rangle = 1$. Note that

$$\langle\psi_E|\zeta^{(m)}\rangle = 0 \tag{15}$$

and

$$[w^{(m)}]^2 + [s^{(m)}]^2 = 1 \tag{16}$$

by definition. What we mean by the SSS equilibrium is that there exists a limit $w^{(eq)}$ defined by

$$\lim_{m_t\to\infty} \frac{1}{m_t} \sum_{m=m_s}^{m_s+m_t-1} w^{(m)} = w^{(eq)}, \qquad (0 < w^{(eq)} \leqslant 1), \tag{17}$$

where $w^{(eq)}$ is independent of m_s whenever m_s is greater than or equal to some value of m.

---

[3] Note that, as was discussed in [7], this average should be calculated with a fixed $\{\{\eta^{(m)}\}, \{\eta^{(m-1)}\}, \ldots, \{\eta^{(1)}\}\}$.
[4] This is the same equilibrium that we called the RSSS equilibrium in [8].

Finally, let us comment on a relation that is useful in the equilibrium in order to extract the value of $E = l - Q$. Using (5), (7) and (13), we obtain

$$
\begin{aligned}
w^{(m+1)} C^{(m+1)} &= \langle \psi_{\mathrm{E}} | \psi^{(m+1)} \rangle \, C^{(m+1)} \\
&= \langle \psi_{\mathrm{E}} | \hat{Q} \hat{M}_{\{\eta^{(m+1)}\}} | \psi^{(m)} \rangle \\
&= \langle \psi_{\mathrm{E}} | \hat{Q} \{ | \psi^{(m)} \rangle + | \chi^{(m)} \rangle g^{(m)} \} \\
&= Q \{ \langle \psi_{\mathrm{E}} | \psi^{(m)} \rangle + \langle \psi_{\mathrm{E}} | \chi^{(m)} \rangle g^{(m)} \} \\
&= Q w^{(m)} + Q \langle \psi_{\mathrm{E}} | \chi^{(m)} \rangle g^{(m)}.
\end{aligned}
\tag{18}
$$

If the second term in the right-hand side is negligible, it leads to

$$
w^{(m+1)} \simeq \frac{Q}{C^{(m+1)}} w^{(m)}.
\tag{19}
$$

Then, in the equilibrium where $w^{(m)} \simeq w^{(m+1)} \simeq w^{(\mathrm{eq})} \neq 0$ for sufficiently large values of m, we can expect

$$
Q \simeq C^{(m+1)}.
\tag{20}
$$

Thus we become aware that the value of E can be estimated from the normalization factor $C^{(m+1)}$.

3. Existence of the SSS equilibrium

In this section we present analytic and qualitative discussions on the existence of the SSS equilibrium. This section consists of three subsections. The first subsection gives some equations for $C^{(m+1)}$ assuming that fluctuations can be neglected. The next subsection is devoted to summarized discussions for unfrustrated systems, where all elements of the operator $\hat{Q}$ are non-negative [8]. In the third subsection we show that the SSS equilibrium also exists for frustrated systems when the parameter ϵ is small enough.

3.1. An equation for the equilibrium

We pay our attention to a relation leading from (5), (7) and (12):

$$
\begin{aligned}
| \psi^{(m+1)} \rangle C^{(m+1)} &= \hat{Q} \hat{M}_{\{\eta^{(m+1)}\}} | \psi^{(m)} \rangle \\
&= Q | \psi_{\mathrm{E}} \rangle w^{(m)} + \hat{Q} | \zeta^{(m)} \rangle s^{(m)} + \hat{Q} | \chi^{(m)} \rangle g^{(m)}.
\end{aligned}
\tag{21}
$$

With normalization conditions and (15) and (16), this yields

$$
\begin{aligned}
[C^{(m+1)}]^2 = {} & Q^2 [w^{(m)}]^2 \\
& + \langle \zeta^{(m)} | \hat{Q}^2 | \zeta^{(m)} \rangle (1 - [w^{(m)}]^2) + \langle \chi^{(m)} | \hat{Q}^2 | \chi^{(m)} \rangle [g^{(m)}]^2 \\
& + 2 Q^2 w^{(m)} \langle \psi_{\mathrm{E}} | \chi^{(m)} \rangle g^{(m)} + 2 s^{(m)} \langle \zeta^{(m)} | \hat{Q}^2 | \chi^{(m)} \rangle g^{(m)}.
\end{aligned}
\tag{22}
$$

We assume that both $\langle \zeta^{(m)} | \hat{Q}^2 | \zeta^{(m)} \rangle$ and $\langle \chi^{(m)} | \hat{Q}^2 | \chi^{(m)} \rangle$ are independent of m when m is large enough,

$$
\langle \zeta^{(m)} | \hat{Q}^2 | \zeta^{(m)} \rangle \simeq Q_{2\zeta},
\tag{23}
$$

$$
\langle \chi^{(m)} | \hat{Q}^2 | \chi^{(m)} \rangle \simeq Q_{2\chi},
\tag{24}
$$

where $Q_{2\zeta}$ and $Q_{2\chi}$ denote positive constants. It should be noted that both $Q_{2\zeta}$ and $Q_{2\chi}$ are always less than Q^2, because $Q^2 = \langle \psi_{\mathrm{E}} | \hat{Q}^2 | \psi_{\mathrm{E}} \rangle$ is the largest one among $\langle \psi | \hat{Q}^2 | \psi \rangle$ by definition. We also assume that both of the cross terms in (22) are negligible, noting that statistical averages of them vanish. Thus we obtain a relation

$$
[C^{(m+1)}]^2 \simeq Q^2 [w^{(m)}]^2 + Q_{2\zeta} (1 - [w^{(m)}]^2) + Q_{2\chi} [g^{(m)}]^2.
\tag{25}
$$

Let us here emphasize that $[g^{(m)}]^2$ measures the degree of the difference between $|\psi^{(m)}\rangle$ and $\hat{M}_{\{\eta^{(m+1)}\}}|\psi^{(m)}\rangle$. We would like to note again that the statistical average of $[g^{(m)}]^2$ is calculated from coefficients for $|\psi^{(m)}\rangle$ and the parameter ϵ (see (10)).

3.2. The equilibrium in unfrustrated systems

Here we briefly comment how we conclude that the SSS equilibrium should exist in unfrustrated cases with any value of ϵ. Detailed discussions and several numerical examinations with the J_1–J_2 Heisenberg model ($J_2/J_1 = 0, -1$) are presented in [8]. In this subsection we limit ourselves to the case $|\psi^{(0)}\rangle = |\psi_E\rangle$ in order to make our analysis clear. Discussions for a good approximate initial trial state can be made in a similar manner.

For unfrustrated systems it is always possible to choose an adequate basis $\{|i\rangle\}$ for which all f_i s in $|\psi_E\rangle \equiv \sum_i |i\rangle f_i$ as well as $q_{ij} \equiv \langle i|\hat{Q}|j\rangle$ s are non-negative. Note that all coefficients in the expansion of $|\psi^{(1)}\rangle, |\psi^{(2)}\rangle, \ldots$ are then also non-negative. This is because, in the relation we learn from (5),

$$c_i^{(m)} = \sum_j q_{ij} c_j^{(m-1)} \eta_j^{(m)} / C^{(m)}, \tag{26}$$

$q_{ij} \geqslant 0$ for all i and j and $\eta_j^{(m)}/C^{(m)} \geqslant 0$ for all j by definition. Let us then examine the first term in (10). One upper bound for it is given by

$$\epsilon \sum_{|c_i^{(m)}|<\epsilon} |c_i^{(m)}| \leqslant \epsilon \sum_i |c_i^{(m)}| = \epsilon \sum_i c_i^{(m)}, \tag{27}$$

where the last equality follows from the fact that all $c_i^{(m)}$ are non-negative here. Further, we can expect that, in positive definite cases,

$$\epsilon \sum_i c_i^{(m)} \sim w^{(m)} \epsilon \sum_i f_i \tag{28}$$

holds for any m [8]. Now we add one more assumption in order to propose clearly a relation that is to be expected in the SSS equilibrium. Noting that $\sum_m [c_i^{(m)}]^2 = 1$, we assume for the second term of (10) that

$$\sum_{|c_i^{(m)}|<\epsilon} [c_i^{(m)}]^2 \simeq K \tag{29}$$

holds with sufficiently large values of m, where K ($0 < K \leqslant 1$) is a constant defined by ϵ. This brings, together with (28), a relation

$$[g^{(m)}]^2 \simeq G w^{(m)} - K, \qquad G \equiv \epsilon \sum_i f_i. \tag{30}$$

Combining (19), (25) and (30), we obtain a recursive relation for $w^{(m)}$:

$$w^{(m+1)} \simeq \frac{Q w^{(m)}}{\sqrt{(Q^2 - Q_{2\zeta})[w^{(m)}]^2 + G Q_{2\chi} w^{(m)} + (Q_{2\zeta} - K Q_{2\chi})}}. \tag{31}$$

A simple mathematical analysis based on (31) [8] leads us to the conclusion that $w^{(eq)}$ exists as far as $G > K$ and $Q_{2\zeta} > K Q_{2\chi}$.[5] Also, it is concluded that $w^{(eq)}$ should satisfy a quadratic equation for w:

$$(Q^2 - Q_{2\zeta})w^2 + G Q_{2\chi} w - (Q^2 - Q_{2\zeta} + K Q_{2\chi}) = 0. \tag{32}$$

---

[5]   We observed that these conditions are fulfilled for any value of ϵ that we have studied.

The relevant solution which belongs to the interval (0, 1] is

$$w^{(\text{eq})} = -q + \sqrt{q^2 + 1 + \kappa}, \qquad q \equiv \frac{1}{2} \cdot \frac{G Q_{2\chi}}{Q^2 - Q_{2\zeta}} (> 0), \qquad \kappa \equiv \frac{K Q_{2\chi}}{Q^2 - Q_{2\zeta}} (> 0).$$

(33)

Thus we come to the conclusion that the SSS equilibrium exists in unfrustrated systems.

3.3. The equilibrium in frustrated systems

In this subsection we show that the SSS equilibrium should, at least for small values of ϵ, also exist for frustrated systems.

Let us find an equation for $w^{(\text{eq})}$ in frustrated systems from (25). We again start from examining $[g^{(m)}]^2$, with an assumption that it becomes almost constant ($\equiv g^2$) for sufficiently large values of m. Then (10) brings an upper bound,

$$g^2 \simeq [g^{(m)}]^2 \simeq \langle\!\langle [g^{(m)}]^2 \rangle\!\rangle \leqslant \epsilon \sum_{|c_i^{(m)}| < \epsilon} |c_i^{(m)}| \leqslant \epsilon \sum_{i=1}^{N_V} |c_i^{(m)}| \leqslant \epsilon \sqrt{N_V}.$$

(34)

The last inequality is based on the fact that $\max_{\sum c_i^2 = 1} \sum |c_i| = \sqrt{N_V}$.

If the SSS equilibrium exists, $w^{(\text{eq})}$ should satisfy the following equation for w,

$$(Q^2 - Q_{2\zeta})(1 - w^2) \simeq Q_{2\chi} g^2,$$

(35)

which we obtain using (20) and (25). Clearly this equation, where $Q^2 - Q_{2\zeta} > 0$ and $Q_{2\chi} \geqslant 0$ always hold by definition, has a relevant solution if $Q_{2\chi} g^2$ is less than $Q^2 - Q_{2\zeta}$. Because of the upper bound (34), we then see that there exists a solution

$$w^{(\text{eq})} = \sqrt{1 - \frac{Q_{2\chi} g^2}{Q^2 - Q_{2\zeta}}}, \qquad (0 < w^{(\text{eq})} \leqslant 1)$$

(36)

for small values of ϵ. Therefore we conclude that the SSS equilibrium is realized in frustrated systems when the value of the parameter ϵ is small enough.

4. Numerical study

Now we present numerical results on the frustrated J_1–J_2 Heisenberg model. The Hamiltonian of the model is

$$\hat{H}_{J_1 J_2} \equiv J_1 \sum_{(nn)} \mathbf{S}_i \cdot \mathbf{S}_j + J_2 \sum_{(nnn)} \mathbf{S}_i \cdot \mathbf{S}_{j'}.$$

(37)

Here $\mathbf{S}_k$ denotes the spin-$1/2$ operator on the site k and summations run over the nearest-neighbour pairs (nn) or over the next-nearest-neighbour pairs (nnn) of the square lattice. In this work we restrict ourselves to the $S_z = 0$ sector, where S_z denotes the z component of the total spin[6]. Values of couplings are fixed to be $J_1 = 1$ and $J_2 = 0.5$ throughout this paper.

As is mentioned in section 2, the value of l in the operator $\hat{Q} \equiv l\hat{I} - \hat{H}_{J_1 J_2}$ should be determined to make the largest eigenvalue for $\hat{Q}$ correspond to the lowest eigenvalue of $\hat{H}_{J_1 J_2}$, which we denote by E. Since the largest eigenvalue of $\hat{H}_{J_1 J_2}$ on an N_s-site lattice is $2(J_1 + J_2)N_s/4$ with the largest $S_z(= N_s/2)$, this means a condition $2l > (J_1 + J_2)N_s/2 - |E|$. Also keep in mind that a very large value of l should be avoided, because it causes slow

---

[6] A study with other symmetries is also possible. For example, we study both $S_z = 0$ and $S_z = 1$ sectors in [6, 7].
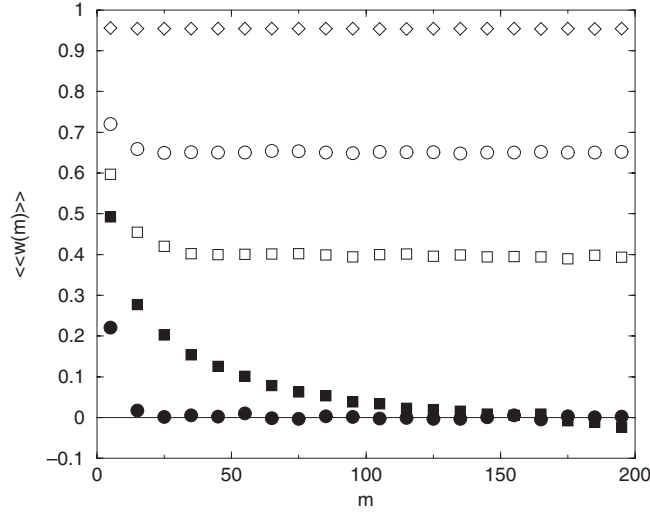
Figure 1. Statistical averages for $w^{(m)}$ on the 20-site lattice with $\epsilon = 0.05$ (filled circles), 0.025 (filled squares), 0.02 (open squares), 0.015 (open circles) and 0.005 (open diamonds).

convergence. Values of l thus chosen for each lattice size with a guess for E will be given in each subsection.

This section, which includes three subsections, is for numerical studies on lattices up to $N_s = 40$. In the first subsection we make a detailed study of the SSS equilibrium on an $N_s = 20$ lattice. Comparing our results with those obtained from the exact eigenstate, we demonstrate that our assumptions described in the previous section are reasonable. In the second subsection we evaluate the lowest energy eigenvalue on $N_s = 32$ and 36 lattices, imposing some symmetries on their bases. We will see that our results are in good agreement with the known exact ground-state energy. The third subsection is for the $N_s = 40$ results.

4.1. $N_s = 20$ results

For this lattice size there are $_{20}C_{10} = 184, 756$ configurations which fulfill the condition $S_z = 0$. We use these configurations as basis states $|i\rangle$, without assuming any symmetry on the state $|\psi^{(m)}\rangle$. Let $\hat{Q} \equiv 3\hat{I} - \hat{H}_{J_1 J_2}$ in this subsection. It is easy to carry out the exact diagonalization of the matrix $[\langle i|\hat{Q}|j\rangle]$ and find the exact eigenstate $|\psi_E\rangle$. Remember that $\hat{Q}|\psi_E\rangle = Q|\psi_E\rangle$ and Q is the eigenvalue for which the value of $|Q|$ is the largest among all eigenvalues for $\hat{Q}$. Numerically, we obtain $Q = 13.0123$, which certainly reproduces the exact ground-state energy of the system.

In this subsection we start from the exact eigenstate, namely $|\psi^{(0)}\rangle = |\psi_E\rangle$. Then, according to (5), we sequentially calculate $|\psi^{(m)}\rangle$ up to $m = 200$. Figures 1–6 present results on several quantities described in previous sections. All statistical averages in these figures are calculated from ten samples for each value of ϵ. We do not plot statistical errors, because they are scarcely beyond the marks that we have used in the figures.

In figure 1 we present the results on $w^{(m)} \equiv \langle\psi_E|\psi^{(m)}\rangle$ for several values of ϵ as a function of m. We see that, for each value of ϵ less than or equal to 0.02, $w^{(m)}(m > \sim 30)$ fluctuates around a finite value defined by ϵ. This is the very evidence for the SSS equilibrium. Meanwhile, when $\epsilon \geqslant 0.025$, $w^{(m)}$ decreases rapidly to zero as m grows. Therefore no SSS equilibrium takes place in this parameter region. Figure 2 shows the normalization factor $C^{(m)}$
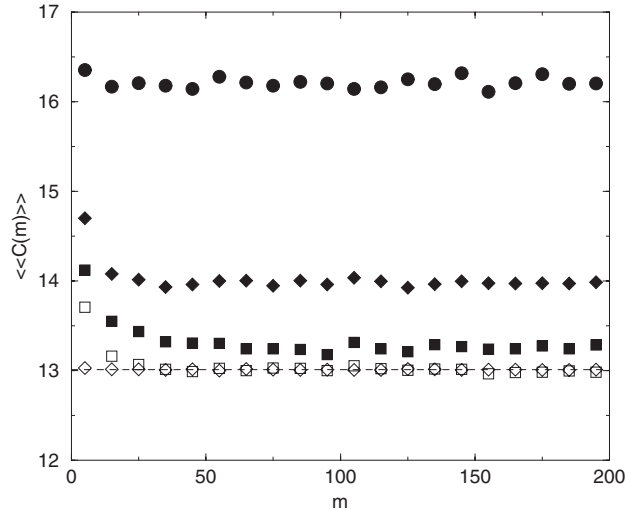
Figure 2. Statistical averages for $C^{(m)}$ on the 20-site lattice with $\epsilon = 0.05$ (filled circles), 0.03 (filled diamonds), 0.025 (filled squares), 0.02 (open squares) and 0.005 (open diamonds). The dashed line indicates the eigenvalue $Q(= 3 - E) = 13.0123$.
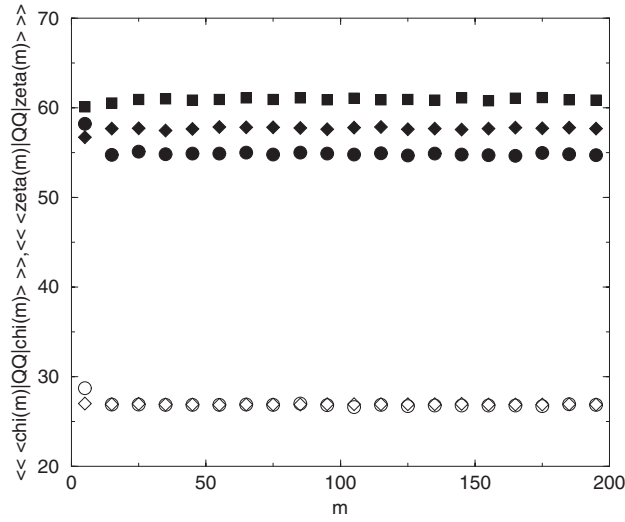

Figure 3. Statistical averages for $\langle \zeta^{(m)} | \hat{Q}^2 | \zeta^{(m)} \rangle$ (filled marks) and $\langle \chi^{(m)} | \hat{Q}^2 | \chi^{(m)} \rangle$ (open marks) on the 20-site lattice. Circles, squares and diamonds show the data with $\epsilon = 0.05$, 0.02 and 0.005, respectively.

that we calculate from (6). Our results in figure 2 confirm that values of $C^{(m)}$ are around the exact eigenvalue Q when the SSS equilibrium occurs.

Figures 3–5 are to endorse relations (23), (24) and (25). In figure 3 we plot values of $\langle \zeta^{(m)} | \hat{Q}^2 | \zeta^{(m)} \rangle$ and $\langle \chi^{(m)} | \hat{Q}^2 | \chi^{(m)} \rangle$ for some values of ϵ. It is clear that our assumptions (23) and (24) are both acceptable, because $\langle \zeta^{(m)} | \hat{Q}^2 | \zeta^{(m)} \rangle$ and $\langle \chi^{(m)} | \hat{Q}^2 | \chi^{(m)} \rangle$ hardly depend on m when $m > \sim 20$. We also observe that (23) and (24) hold for other values of ϵ. The resultant
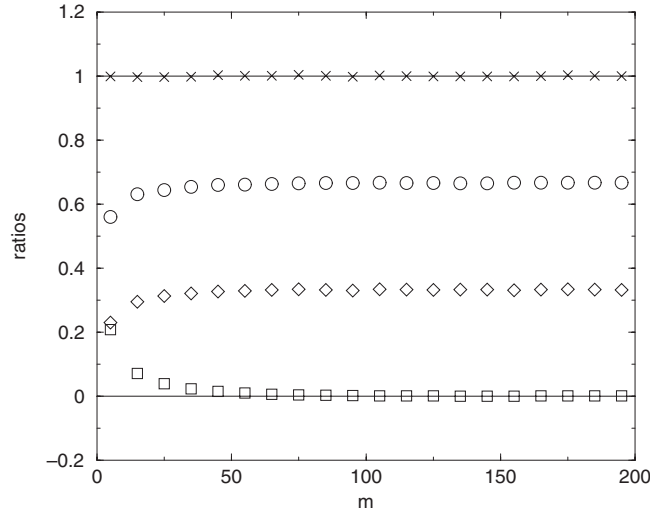
Figure 4. Ratios $Q^2[w^{(m)}]^2/[C^{(m+1)}]^2$ (squares), $Q_{2\zeta}(1 - [w^{(m)}]^2)/[C^{(m+1)}]^2$ (diamonds), $Q_{2\chi}[g^{(m)}]^2/[C^{(m+1)}]^2$ (circles) and $\{Q^2[w^{(m)}]^2 + Q_{2\zeta}(1 - [w^{(m)}]^2) + Q_{2\chi}[g^{(m)}]^2\}/[C^{(m+1)}]^2$ (crosses) on the 20-site lattice with $\epsilon = 0.025$.
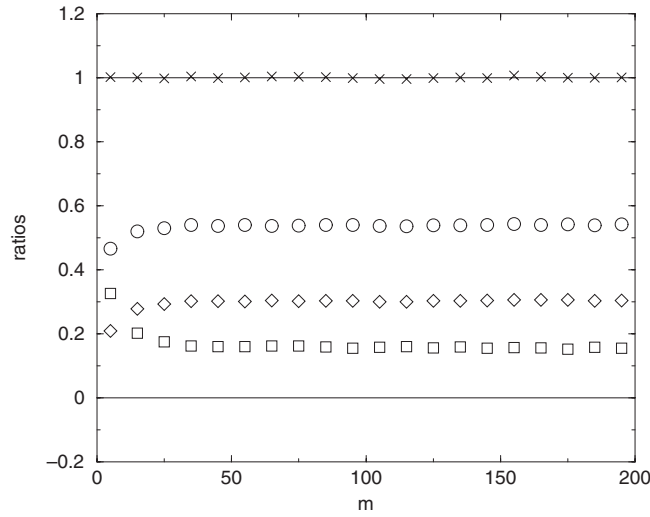

Figure 5. Ratios $Q^2[w^{(m)}]^2/[C^{(m+1)}]^2$ (squares), $Q_{2\zeta}(1 - [w^{(m)}]^2)/[C^{(m+1)}]^2$ (diamonds), $Q_{2\chi}[g^{(m)}]^2/[C^{(m+1)}]^2$ (circles) and $\{Q^2[w^{(m)}]^2 + Q_{2\zeta}(1 - [w^{(m)}]^2) + Q_{2\chi}[g^{(m)}]^2\}/[C^{(m+1)}]^2$ (crosses) on the 20-site lattice with $\epsilon = 0.02$.

value of $Q_{2\zeta}$ ($Q_{2\chi}$) first increases (decreases), then decreases (increases), as we lessen the value of ϵ. The change for $Q_{2\chi}$ is, however, too small to read in this figure. Figures 4 and 5 present ratios of three terms in the right-hand side of (25) to $[C^{(m+1)}]^2$ for $\epsilon = 0.025$, where no equilibrium is observed, and for $\epsilon = 0.02$ with which the system realizes the equilibrium. We see that the sum of the three ratios for each m is in good agreement with the expected value, namely 1.0. We also observe such agreements for other values of ϵ. Therefore we can say that the relation (25) is acceptable regardless of the equilibrium. In other words, we can conclude
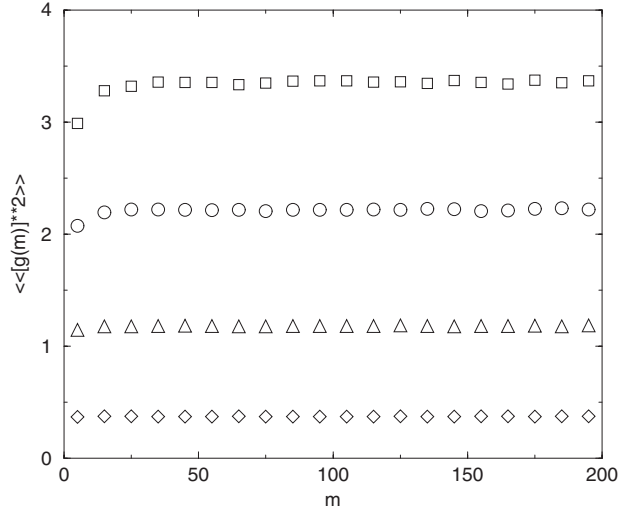
Figure 6. Statistical averages for $[g^{(m)}]^2$ on the 20-site lattice as a function of m. Squares, circles, triangles and diamonds show the data with $\epsilon = 0.02, 0.015, 0.01$ and 0.005, respectively.

that the cross terms $2Q^2 w^{(m)}\langle\psi_E|\chi^{(m)}\rangle g^{(m)}$ and $2s^{(m)}\langle\zeta^{(m)}|\hat{Q}^2|\chi^{(m)}\rangle g^{(m)}$ in (22) are always negligible for this system.

Let us next examine the relation (36) in the SSS equilibrium. Figure 6 plots $\langle\!\langle[g^{(m)}]^2\rangle\!\rangle$ with $\epsilon = 0.02, 0.015, 0.01$ and 0.005. We see, in accordance with what we have assumed at the beginning of (34), that fluctuations in $[g^{(m)}]^2$ due to different random number sequences are negligibly small and that $[g^{(m)}]^2$ for each value of ϵ becomes almost irrelevant to m for $m > {\sim}20$. For any value of ϵ shown in figure 6, we observe that the value of $w^{(eq)}$ estimated from $\sqrt{1 - \langle\!\langle\langle\chi^{(m)}|\hat{Q}^2|\chi^{(m)}\rangle\rangle\!\rangle\langle\!\langle[g^{(m)}]^2\rangle\!\rangle/(Q^2 - \langle\!\langle\langle\zeta^{(m)}|\hat{Q}^2|\zeta^{(m)}\rangle\rangle\!\rangle)}$ is in good agreement with values of $\langle\!\langle w^{(m)}\rangle\!\rangle$ in figure 1.

Finally, we comment on how many basis states should be included in our calculation. As a result of the stochastic state selection, $N_a^{(m)}$, the number of non-zero coefficients in the expansion of $\hat{M}_{\{\eta^{(m+1)}\}}|\psi^{(m)}\rangle$, is much less than $N_b^{(m)}$, the number of non-zero coefficients in the expansion of $|\psi^{(m)}\rangle$. Hence it is not $N_a^{(m)}$ but $N_b^{(m)}$ that determines the necessary memory resources. For each value of ϵ we observe that, after several iterative operations to generate $\hat{Q}\hat{M}_{\{\eta^{(m)}\}}|\psi^{(m-1)}\rangle(= C^{(m)}|\psi^{(m)}\rangle)$, $N_b^{(m)}$ does not increase anymore. The data also show very small deviations for different random number sequences. Therefore the upper limit of $N_b^{(m)}$, which is dependent on the value of ϵ, is critical for the numerical study. Some results for the 20-site system are as follows. When $\epsilon = 0.05$ the upper limit of $N_b^{(m)}$ is slightly less than 1×10^5, namely we can do with only one half of the $N_V = 184,756$ basis states. With the value $\epsilon = 0.02$, for which the system exhibits the SSS equilibrium, we need about 80% of the N_V. The ratio $N_b^{(m)}/N_V$ amounts to about 0.88 if we employ the value $\epsilon = 0.01$.

4.2. $N_s = 32$ and 36 results

Here we concentrate on the zero-momentum states which are even under rotations and reflections. Based on these conditions, we construct a basis that possesses translation, rotation and reflection symmetries of the lattice [11]. The total numbers of $S_z = 0$ basis states are then ${\sim}2.4 \times 10^6$ and ${\sim}3.2 \times 10^7$ for the $N_s = 32$ and 36 lattices, respectively. Since we can employ
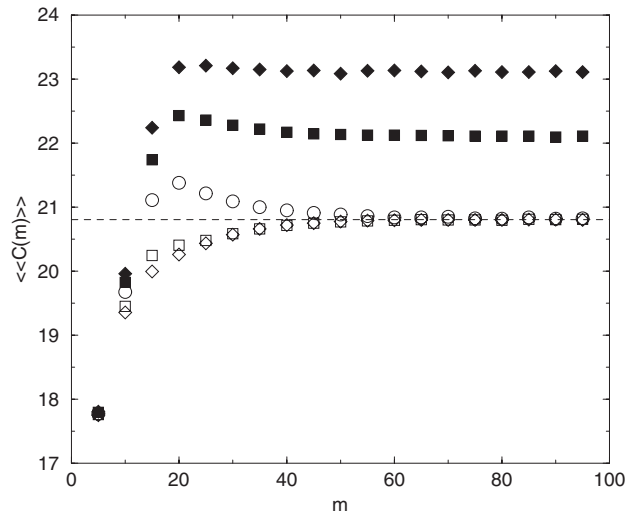
Figure 7. Statistical averages for $C^{(m)}$ on the 32-site lattice as a function of m, where each average is calculated from 30 samples. Filled diamonds, filled squares, open circles, open squares and open diamonds show the data with $\epsilon = 0.015$, 0.013, 0.010, 0.005 and 0.0025, respectively. The dashed line indicates the value $4.8 - E = 20.8031$ [11].
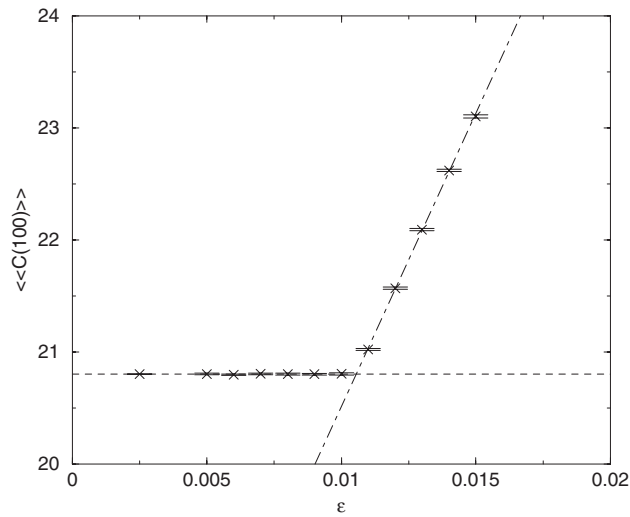

Figure 8. Statistical averages for $C^{(100)}$ on the 32-site lattice as a function of ϵ. Each average is calculated from 30 samples. The dashed line indicates the value $4.8 - E = 20.8031$ [11] and the dot–dashed line shows the result from the linear fit for data with $0.01 < \epsilon \leqslant 0.015$.

any initial trial state as long as it has some overlap with the exact eigenstate, we start from the Néel state for simplicity. The value of l in the operator $\hat{Q} = l\hat{I} - \hat{H}_{J_1 J_2}$ is set to be 4.8 (5.4) for the 32-site (36-site) lattice, so that the largest eigenvalue for $\hat{Q}$ gives the lowest eigenvalue of $\hat{H}_{J_1 J_2}$.

Let us first report results on the 32-site lattice. Changing values of ϵ, we calculate $\langle\langle C^{(m)} \rangle\rangle$ ($m \leqslant 100$) from 30 samples for each value of ϵ. Figures 7 and 8 present the results, where
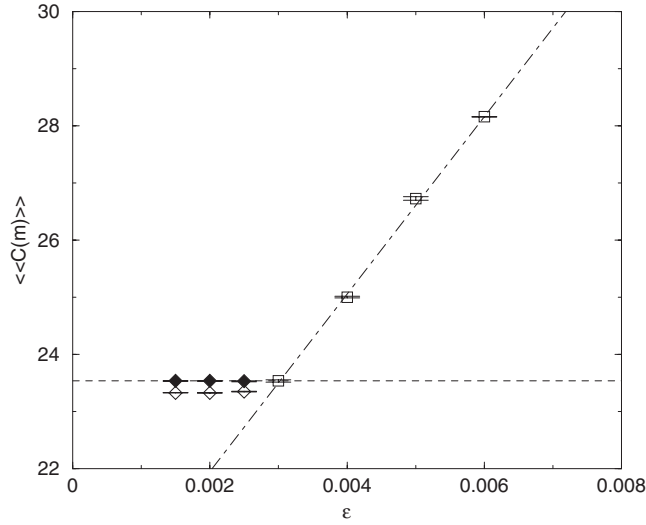
Figure 9. Statistical averages for $C^{(40)}$ (open squares, open diamonds) and $C^{(100)}$ (filled diamonds) on the 36-site lattice as a function of ϵ. Each average for $\epsilon \leqslant 0.0025$ (the open diamond or the filled diamond) is calculated from 20 samples, while each average for $\epsilon \geqslant 0.003$ (the open square) is calculated from two samples. The dashed line indicates the value of $5.4 - E = 23.5372$ [11]. The dot–dashed line shows the result from the least-squares fit for data with $0.003 \leqslant \epsilon \leqslant 0.006$.

statistical errors are so small that we omit them. In figure 7 the results are shown as a function of m. We see that the data become almost constant when $m > \sim 50$. Figure 8 plots values of $\langle\!\langle C^{(100)} \rangle\!\rangle$ as a function of ϵ. A linear decrease to meet a kink at $\epsilon \sim 0.01$ is observed in the figure, and below this value the results are almost constant. We therefore come to the conclusion that the SSS equilibrium manifests itself when $\epsilon \leqslant 0.01$, and that measurements of the normalization factors $C^{(m)}$ in this parameter range enable us to estimate the lowest energy eigenvalue of the system[7]. We observe that the estimated values from $\langle\!\langle C^{(100)} \rangle\!\rangle$ with $\epsilon = 0.01$ and $\epsilon = 0.0025$ are $E = -16.0052 \pm 0.0092$ and $E = -16.0047 \pm 0.0028$, respectively. These values are in good agreement with $E = -16.0031$, the exact ground-state energy obtained from [11]. The upper bound of $N_{\mathrm{b}}^{(m)}$ is $\sim 1.7 \times 10^6$ for $\epsilon = 0.01$, $\sim 1.8 \times 10^6$ for $\epsilon = 0.005$ and $\sim 1.9 \times 10^6$ for $\epsilon = 0.0025$, that is, about 73%, 77% and 81% of N_{V}.

The results on the 36-site lattice are qualitatively similar to those on the 32-site lattice. In figure 9 we show $\langle\!\langle C^{(40)} \rangle\!\rangle$ for $0.0015 \leqslant \epsilon \leqslant 0.006$ as well as $\langle\!\langle C^{(100)} \rangle\!\rangle$ for $0.0015 \leqslant \epsilon \leqslant 0.0025$. We observe a linear dependence of $\langle\!\langle C^{(40)} \rangle\!\rangle$ on ϵ in the range $0.003 \leqslant \epsilon \leqslant 0.006$, while data with smaller values of ϵ are almost constant. This kind of stability is observed with both $\langle\!\langle C^{(40)} \rangle\!\rangle$ and $\langle\!\langle C^{(100)} \rangle\!\rangle$ for $\epsilon \leqslant 0.0025$, although the value of the constant is slightly different, as we see in the figure. From 20 samples of $\langle\!\langle C^{(100)} \rangle\!\rangle$ with $\epsilon = 0.0025, 0.002$ and 0.0015, we obtain $E = -18.1317 \pm 0.0089, -18.1357 \pm 0.0048$ and -18.1364 ± 0.0028, respectively. Within the statistical errors, they all agree with the known exact ground-state energy $E = -18.1372$ [11]. The upper bound of $N_{\mathrm{b}}^{(m)}$ (ratio to N_{V}) is about 2.4×10^7 (0.75) when $\epsilon = 0.0015$.

---

[7] It should be kept in mind that all we can estimate here is, of course, the lowest energy eigenvalue in the sector which has the same symmetries as our basis.
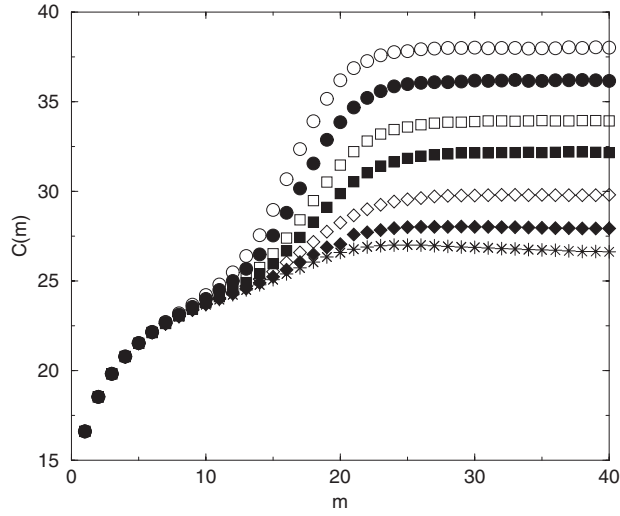
Figure 10. Values of $C^{(m)}$ on the 40-site lattice for $\epsilon \geqslant 0.001$ as a function of m. The initial trial state is the Néel state. Open circles, filled circles, open squares, filled squares, open diamonds, filled diamonds and asterisks denote data with $\epsilon = 0.005, 0.0035, 0.0025, 0.002, 0.0015, 0.0012$ and 0.001, respectively.

4.3. $N_s = 40$ results

In this subsection we show results on a 40-site lattice. Since this lattice lacks the reflection symmetry, we employ a basis which possesses the up-down symmetry of spins in addition to the translation and rotation symmetries of the lattice. The size of the full vector space with $S_z = 0$ is then $N_V \simeq 4.3 \times 10^8$. We define $\hat{Q} \equiv 6\hat{I} - \hat{H}_{J_1 J_2}$ in this subsection.

For $\epsilon \geqslant 0.001$ we calculate $C^{(m)}$ starting from the Néel state. In the range $\epsilon \geqslant 0.002$, two samples are calculated for each value of ϵ. We observe that deviations of $C^{(m)}$ between different random number sequences are very small; the statistical errors are 0.5% at most. Since our data from one sample would have enough precision for this system, only one sample is calculated for each value of ϵ that is less than 0.002. Figure 10 shows some of the results for $\epsilon \geqslant 0.001$, where we present data from each sample as a function of m. We see that $C^{(m)}$ ($m \geqslant 30$) for each value of ϵ becomes almost constant when $\epsilon \geqslant 0.0012$. For $\epsilon = 0.001$, on the other hand, $C^{(m)}$ is still decreasing at $m = 40$. We therefore continue to calculate $C^{(m)}$ with $\epsilon = 0.001$ up to $m = 65$. The values that we obtain are $C^{(40)} = 26.620$ and $C^{(65)} = 26.417$.

In further calculations of $C^{(m)}$ with $\epsilon = 0.0008$, we employ a better trial state which is constructed in the same manner as that in [9]. Values of $C^{(m)}$ thus obtained are presented in figure 11. The upper bound of $N_b^{(m)}$ is $\sim 3.3 \times 10^8$ (76% of N_V).

In figure 12 we plot values of $C^{(40)}$ (for $0.001 < \epsilon \leqslant 0.0025$), the value of $C^{(65)}$ (for $\epsilon = 0.001$) and the value of $C^{(50)}$ (for $\epsilon = 0.0008$) as a function of ϵ. We see that the datum with $\epsilon = 0.0008$ is located above the line in the figure which is determined by data between $\epsilon = 0.001$ and 0.0015. Therefore, for the same reason as in the 32-site and 36-site cases, we conclude that the 40-site system realizes the SSS equilibrium when $\epsilon = 0.0008$.

In order to evaluate the lowest energy of the system without any statistical average, we attempt to find a zone which should include the true energy eigenvalue. The upper (lower) value of this zone is determined by the maximum (minimum) value of $C^{(m)}$ with $m \geqslant m_e$, where m_e denotes a value of m above which the system is in the SSS equilibrium. This approach seems
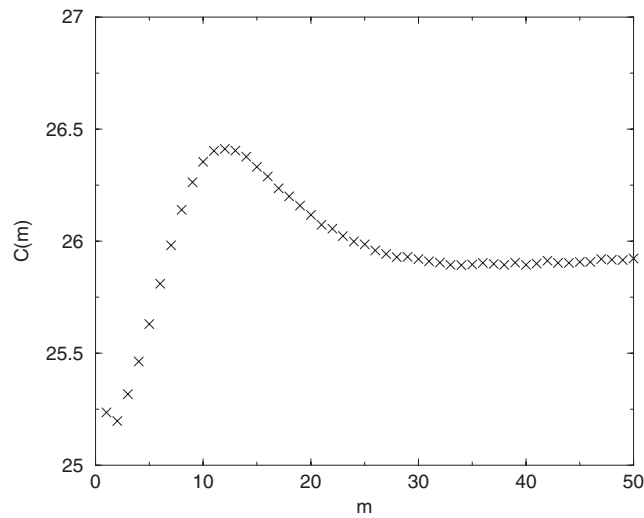
14

Figure 11. Values of $C^{(m)}$ on the 40-site lattice with $\epsilon = 0.0008$ as a function of m. The initial trial state is an approximate ground state which yields $\langle \psi^{(0)} | \hat{Q} | \psi^{(0)} \rangle = \langle \psi^{(0)} | 6\hat{I} - \hat{H} | \psi^{(0)} \rangle = 18.814$.
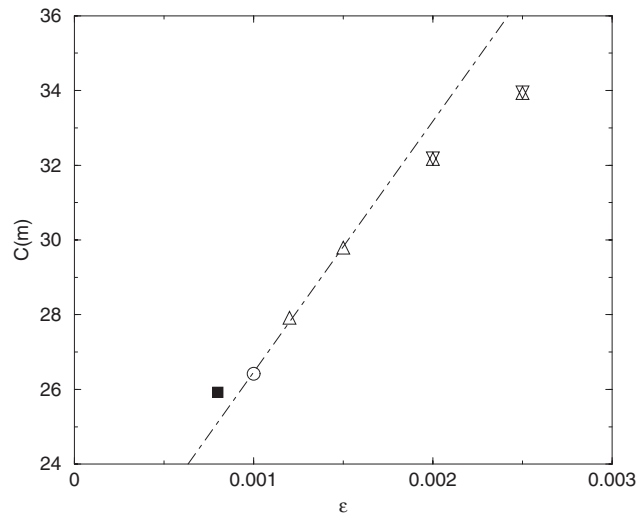

Figure 12. Values of $C^{(40)}$ (open triangles), $C^{(50)}$ (the filled square) and $C^{(65)}$ (the open circle) on the 40-site lattice as a function of ϵ. Each datum is obtained from one sample. The dot–dashed line shows the result from the least-squares fit for data with $0.001 \leqslant \epsilon \leqslant 0.0015$.

to work nicely in the 32-site and the 36-site systems, resultant zones being much wider than the stripes obtained using the statistical treatments[8]. Our best estimate for the zone in the 40-site system is $-19.92 \leqslant E \leqslant -19.89$, which we obtain from values of $C^{(m)}$ with $\epsilon = 0.0008$ and $m_e = 40 \leqslant m \leqslant 50$.

---

[8] In the 36-site case, for example, the zone obtained from one sample with $\epsilon = 0.002$ and $m_e = 60 \leqslant m \leqslant 100$ is $23.4964 \leqslant Q \leqslant 23.5563$. This is equivalent to $-18.1563 \leqslant E \leqslant -18.0964$. This includes a stripe $-18.1405 \leqslant E \leqslant -18.1309$ ($E = -18.1357 \pm 0.0048$), which is the value that we obtained in the previous subsection.

5. Summary and discussions

In this paper we have studied a frustrated quantum spin model using the SSS (stochastic state selection) method. Our purpose is to see whether the SSS equilibrium [8], a kind of equilibrium which we have found in a study of quantum spin models with positive-definite Hamiltonians, is also realized in frustrated systems.

In the SSS method we start from an initial trial state and recursively calculate the mth normalized intermediate state ($m = 1, 2, 3, \ldots$). Each generating procedure is as follows. First we operate the mth random choice operator to the $(m - 1)$th normalized intermediate state. By this operation, the effective size of the vector space is drastically reduced. The rate of reduction is controlled by a parameter ϵ. Then, successively, we operate $\hat{Q} \equiv l\hat{I} - \hat{H}$ to the reduced state. This operation again increases the number of the basis states that are relevant to the resultant state. Finally, we normalize the state to obtain the mth normalization factor and the mth normalized intermediate state. The system is in the SSS equilibrium if, after repeating the procedure many times, the mth normalized intermediate state comes to contain a finite portion of the ground state and this portion is irrelevant to m. It should be kept in mind that in unfrustrated models the SSS equilibrium is observed for any value of the parameter ϵ.

What we assert for frustrated quantum spin models is that the SSS equilibrium is also realized in these models with *small* values of the parameter ϵ. After analytical arguments in section 3, we present results from numerical calculations for the J_1–J_2 Heisenberg model on 20-, 32-, 36- and 40-site lattices with $J_2/J_1 = 0.5$. We observe that these systems are in the SSS equilibrium in some range of ϵ. We also confirm that in the equilibrium we can effectively estimate the lowest energy eigenvalue of the system. Our results on 20-, 32- and 36-site lattices are in good agreement with the known exact ground-state energies. On a 40-site lattice we obtain the result $-19.92 \leqslant E \leqslant -19.89$, the basis states required for this calculation being maximally 76% of the full vector space. The energy per site is then $-0.4980 \leqslant E/N_s \leqslant -0.4973$, which is greater than the reported values for smaller lattices [11], $E/N_s = -0.503\,810$, $-0.500\,096$ and $-0.500\,615$ for $N_s = 36$, 32 and 20, respectively. Since the value for $N_s = 36$ seems to be irregular, we omit it from the extrapolation. The extrapolation to $N_s \rightarrow \infty$ using our $N_s = 20$, 32 and 40 data yields $-0.4993 \leqslant (E/N_s)_\infty \leqslant -0.4946$.

Several remarks are now in order. First, let us emphasize the wide availability of the SSS method in numerical studies. As we have shown in previous works, the SSS method is applicable to various models with various symmetries and various system sizes, in frustrated cases as well as in unfrustrated cases.

Using this method it is possible to calculate many physical quantities that are given by expectation values of some operators. Essential points of the calculation are as follows. Suppose that we want to calculate an expectation value $\langle \psi | \hat{O} | \psi \rangle$, where $\hat{O}$ is a given operator and $|\psi\rangle$ denotes either the exact eigenstate $|\psi_E\rangle$ or an approximate state $|\psi_A\rangle$. In the SSS method we can generate a state $|\psi\rangle + |\chi\rangle g$ instead of $|\psi\rangle$, where $|\chi\rangle g$ is the stochastically determined random state. Since $|\psi\rangle + |\chi\rangle g$ is described by a smaller number of non-zero coefficients compared to $|\psi\rangle$ itself, the method enables us to calculate $(\langle \psi | + g\langle \chi |)\hat{O}(|\psi\rangle + |\chi'\rangle g')$. Then all we should do in addition is to take a statistical average of this quantity, because a mathematical relation

$$\langle\langle ((\langle \psi | + g\langle \chi |)\hat{O}(|\psi\rangle + |\chi'\rangle g')) \rangle\rangle = \langle \psi | \hat{O} | \psi \rangle$$

follows from basic properties of the random state. In [7], for example, we calculate the static structure factor of the spin-1/2 anti-ferromagnetic Heisenberg model on a 36-site triangular lattice in addition to the $S_z = 0$ and 1 energy eigenvalues.

16

The SSS method provides a fundamental improvement in Monte Carlo techniques. Therefore it is easily combined with lots of established techniques such as the power method [5–7] and the Lanczos method [6, 9]. A study of the stochastic diagonalization by De Raedt and Frick [16] suggests that a combination of the SSS method with the Jacobi method would also be interesting.

How large, then, is the cluster size that we can manage in calculations with the SSS method. It of course depends on the aims and models. In a study of the energy eigenvalue, for instance, our purpose in [5–7, 9] is to obtain the upper bounds of eigenvalues from approximate eigenstates. However, in [8] and in this study we want to evaluate the eigenvalue itself through non-zero overlaps with the exact eigenstate which are realized in the SSS equilibrium. The system sizes of the latter case are generally smaller than those of the former case, because smaller values of the parameter ϵ become necessary.

As for models, in addition to the J_1–J_2 model we have studied the spin-1/2 Heisenberg models on a square lattice up to 64 sites [5, 8], on a triangular lattice up to 48 sites [9], and the Shastry–Sutherland model up to 64 sites [6]. We found that the method is especially effective for the Shastry–Sutherland model. This can be understood because of the very compactness of its low-lying eigenstates, where basis states with relatively large coefficients dominate if a restructured dimer-like basis [17] is employed.

We conclude this paper with a comment whether one can apply our method to other frustrated models. From theoretical points of view, the SSS equilibrium would be observed in most models, because our discussion in section 3 is based on very moderate assumptions. How small the parameter ϵ should be is, however, a model-dependent problem that remains to be clarified in future works. If a system realizes the SSS equilibrium with moderate values of ϵ, it is possible to study many physical properties of the system on large lattices.

References

[1] Richter J, Schulenburg J and Honecker A 2004 *Quantum Magnetism* (*Springer Lecture Notes in Physics* vol 645) ed U Schollwöck, J Richter, D J J Farnell and R F Bishop (Berlin: Springer)
[2] Kashima T and Imada M 2001 *J. Phys. Soc. Japan* **70** 3052
[3] Sorella S 2001 *Phys. Rev.* B **64** 024512
[4] White S R 1992 *Phys. Rev. Lett.* **69** 2863
[5] Munehisa T and Munehisa Y 2003 *J. Phys. Soc. Japan* **72** 2759
[6] Munehisa T and Munehisa Y 2004 *J. Phys. Soc. Japan* **73** 340
[7] Munehisa T and Munehisa Y 2004 *J. Phys. Soc. Japan* **73** 2245
[8] Munehisa T and Munehisa Y 2004 Numerical study for an equilibrium in the recursive stochastic state selection method *Preprint* cond-mat/0403626
[9] Munehisa T and Munehisa Y 2006 *J. Phys.: Condens. Matter* **18** 2327
[10] De Raedt H and von der Linden W 1992 *Phys. Rev.* B **45** 8787
  Riera J and Dagotto E 1993 *Phys. Rev.* B **48** 9515
  Homma M, Mizusaki T and Otsuka T 1995 *Phys. Rev. Lett.* **75** 1284
  Modine N A and Kaxiras E 1996 *Phys. Rev.* B **53** 2546
  Dagotto E, Martins G B, Riera J, Malvezzi A L and Gazza C 1998 *Phys. Rev.* B **58** 12063
[11] Schulz H J, Ziman T A L and Poilblanc D 1996 *J. Physique* I **6** 675

[12] Capriotti L and Sorella S 2000 *Phys. Rev. Lett.* **84** 3173
[13] Capriotti L, Becca F, Parola A and Sorella S 2001 *Phys. Rev. Lett.* **87** 097201
[14] Capriotti L, Fubini A, Roscilde T and Tognetti V 2004 *Phys. Rev. Lett.* **92** 157202
[15] Kotov V N, Oitmaa J, Sushkov O and Weihong Z 2000 *Phil. Mag.* B **80** 1483
[16] De Raedt H and Frick M 1993 *Phys. Rep.* **231** 107
[17] Munehisa T and Munehisa Y 1994 *Phys. Rev.* B **49** 3347
[18] http://wase.urz.uni-magdeburg.de/jschulen/spin/index.html